JACS
JOURNAL OF THE AMERICAN CHEMICAL SOCIETY
Communication
pubs.acs.org/JACS

Easy Excited-State Trapping and Record High T_{TIESST} in a Spin-Crossover Polyanionic Fe^{II} Trimer

Verónica Gómez,[†,#,¶] Cristina Sáenz de Pipaón,[†,#] Pilar Maldonado-Illescas,[†] João Carlos Waerenborgh,[‡] Eddy Martin,[†] Jordi Benet-Buchholz,[†] and José Ramón Galán-Mascarós*[,†,§]

[†]Institute of Chemical Research of Catalonia (ICIQ), Avinguda Paisos Catalans 16, E-43007 Tarragona, Spain
[‡]Centro de Ciências e Tecnologias Nucleares, Instituto Superior Técnico, Universidade de Lisboa, 2695-066 Bobadela LRS, Portugal
[§]Catalan Institution for Research and Advanced Studies (ICREA), Passeig Lluis Companys, 23, E-08010 Barcelona, Spain

Supporting Information

ABSTRACT: Reaction of the polysulfonated triazole ligand L = 4-(1,2,4-triazol-4-yl)ethanedisulfonate) with iron(II) salts in water yields the trimeric species $[Fe_3(\mu\text{-}L)_6(H_2O)_6]^{6-}$. This polyanion, as the dimethylammonium salt, shows a thermally induced spin transition above room temperature for the central Fe position in the trimer with a large hysteresis cycle (>85 K) and remarkably slow dynamics. This allows easy quenching of the metastable high-spin (HS) state via gradual cooling (5 K min^{-1}). Once it is trapped, the HS state remains metastable. Thermal energy is not able to promote relaxation into the low-spin ground state below 215 K, with a characteristic T_{TIESST} = 250 K, the highest temperature ever observed for thermal trapping of an excited spin state in a switchable molecular material.

Iron(II) complexes displaying spin crossover (SCO), a phenomenon in which the spin state of the metal center switches between low spin (LS) and high spin (HS) under external stimuli, are a paradigmatic example of switchable molecular materials.[1−5] The spin transition from diamagnetic S = 0 to paramagnetic S = 2 in octahedral Fe^{II} provokes a dramatic change also in color (from pink/red to white/yellow) and size (increment of 10−15% in the metal-to-ligand bonding distances). Besides, if this transition occurs with hysteresis, a memory effect is conferred. Recently, there is a renaissance of SCO materials in molecular magnetism[6−13] because, in contrast to other bistable species such as single-molecule magnets,[14,15] SCO may occur at room temperature. Thus, SCO appears especially well suited for applications in stimuli-responsive molecular switches for multifunctional materials, memories, electrical circuits, or display devices.[16−28] Most reported complexes with hysteretic SCO are mononuclear or polymeric Fe^{II} compounds, typically with neutral or cationic overall charge. Our group has focused on the search for anionic SCO complexes to increase their processing capabilities when incorporated into hybrid materials. With this in mind, we have prepared sulfonated 1,2,4-triazole derivatives as building blocks.[29,30] Here, we report the SCO behavior of the polyanionic Fe^{II} SCO complex $[Fe_3(\mu\text{-}L)_6(H_2O)_6]^{6-}$ (L^{2-} = 4-(1,2,4-triazol-4-yl)ethanedisulfonate, Figure S1). As the corresponding $(Me_2NH_2)^+$ salt, this complex exhibits a spin transition above room temperature with a very large thermal hysteresis loop. Furthermore, the HS state can be easily trapped when cooling down at rates >5 K min^{-1}, remaining in its metastable state up to the highest temperatures ever observed, close to room temperature.

Reaction of L^{2-} with Fe^{II} in a 3:1 ratio in water yielded a pale pink solution. Single crystals of $(Me_2NH_2)_6[Fe_3(\mu\text{-}L)_6(H_2O)_6]$ (**1**) were isolated by layering the reaction mixture with ethanol. **1** contains the trinuclear polyanion $[Fe_3(\mu\text{-}L)_6(H_2O)_6]^{6-}$, formed by a linear array of octahedral Fe^{II} ions (Fe1−Fe2−Fe1) connected by two triple μ-triazole bridges (Figure 1 and Figure S2). The terminal Fe1 position completes its N_3O_3 hexacoordination with three H_2O molecules in *fac* conformation. The metal-to-ligand distances at 100 K (Table S2) indicate HS configuration for Fe1 (average Fe1−N = 2.13 Å) and LS configuration for Fe2 (average Fe2−N = 1.99 Å). The dangling sulfonate moieties from the ethane groups adopt multiple orientations, participating in a complex weakly hydrogen-bonded network involving the dimethylammonium cations and water molecules. The shortest intermolecular O−O distances are in the 2.6−2.9 Å range (Figure S3).

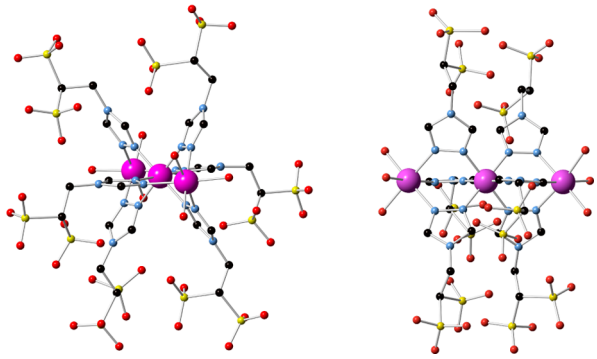

Figure 1. Two views of the molecular structure of $[Fe_3(\mu\text{-}L)_6(H_2O)_6]^{6-}$ (H-atoms omitted for clarity). Color code: Fe = purple; S = yellow; O = red; N = blue; C = black.

Magnetic susceptibility measurements were carried out in the 2−300 K range for grained single crystals of **1** (Figure 2). At room temperature, the $\chi_m T$ product is 6.37 cm^3 mol^{-1} K,

Received: August 3, 2015
Published: September 4, 2015

DOI: 10.1021/jacs.5b07879
J. Am. Chem. Soc. 2015, 137, 11924−11927

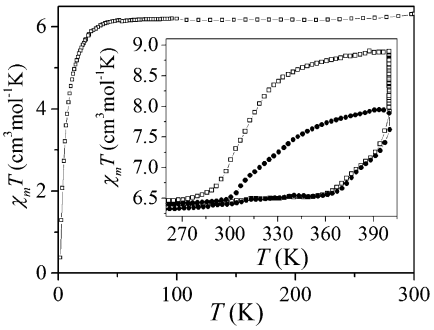

Figure 2. $\chi_m T$ vs T plots for **1** in the 2−300 K range and in the 270−400 K range (inset). Scan rate ≈ 0.1 K min^{-1}. Empty squares show the magnetic behavior when the sample is maintained at 400 K until saturation.

consistent with a HS-LS-HS configuration (spin-only $\chi_m T$ = 6.00 cm^3 mol^{-1} K). On lowering the temperature, $\chi_m T$ remains constant down to 50 K. We assign the rapid decrease below this temperature to zero-field splitting and antiferromagnetic interactions between paramagnetic centers.

Above room temperature (Figure 2, inset), $\chi_m T$ shows a significant increase above 360 K, suggesting a spin transition to the HS-HS-HS state, reaching 7.92 cm^3 mol^{-1} K at 400 K. This corresponds to approximately half of the trimers undergoing spin transition. Upon cooling again, the sample goes slowly back to the HS-LS-HS state, with a hysteresis loop of over 65 K. When the sample is maintained at 400 K, $\chi_m T$ keeps increasing over time until it saturates at 8.89 cm^3 mol^{-1} K (Figure S4), corresponding to ∼84% completeness. The cooling behavior from magnetic saturation at 400 K (Figure 2, inset) exhibits a hysteresis loop of 90 K ($T_{1/2}(\uparrow)$ = 400 K, $T_{1/2}(\downarrow)$ = 310 K), with a quasi-static scan rate. This is among the widest thermal hysteresis ranges found for SCO materials.[31−35] It is also reproducible and robust, as confirmed by the consistency of successive cycles (Figure S5). The possibility of a hydration/dehydration process affecting the hysteretic behavior can be ruled out, given that all measurements were done in perforated capsules to allow proper purging. In addition, analogous behavior was observed for samples previously dehydrated in an oven for 12 h at 135 °C (Figure S5), and thermal gravimetric analysis under humid air (Figure S6) shows no hysteresis related to water content between the cooling and heating branches.

Since SCO can be very sensitive to scan rate,[36,37] we studied its effect in the hysteresis cycle (Figure 3, top). The heating branch does not change significantly with scan rate. The cooling branch deviates at rates faster than 2 K min^{-1}, becoming significantly quenched at scan rates as slow as 5 K min^{-1}. This phenomenon, temperature-induced excited spin-state trapping (TIESST), typically requires very fast cooling (liquid nitrogen immersion),[38−41] with very few exceptions.[42] In the case of **1**, 57% of the complexes are trapped as HS-HS-HS at a 10 K min^{-1} cooling rate. We extracted a characteristic T_{TIESST} = 250 K (Figure 3, bottom) following the method defined by Letard et al.[42] This is the highest T_{TIESST} reported, the previous record being 156 K.[43] At faster heating rates, the HS-HS-HS state is not completely depopulated until reaching room temperature (Figure S7). It is important to note that the X-ray diffraction pattern does not change after multiple thermal cycles, confirming the structural stability of the material (Figure S8).

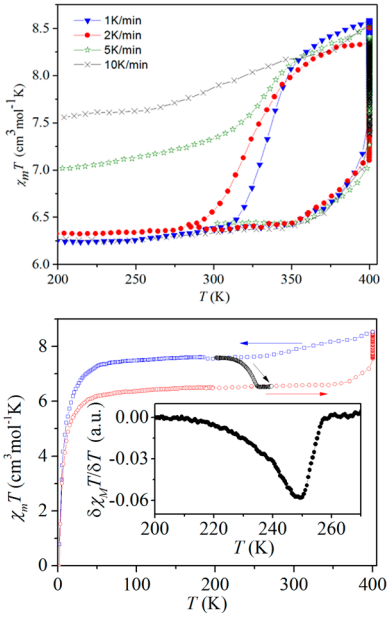

Figure 3. $\chi_m T$ vs T plots for **1** at (top) different heating/cooling rates, allowing for saturation at 400 K, and (bottom) heating up to 400 K until saturation (red circles), cooling down at 10 K min^{-1} (blue circles), and warming up again at 0.3 K min^{-1} (black circles). Inset: $\delta(\chi_m T)/\delta T$ vs T curve for the latter heating branch.

Isothermal relaxation curves (Figure 4), after keeping **1** at 400 K for 6.5 h and then cooling at 10 K min^{-1} down to the

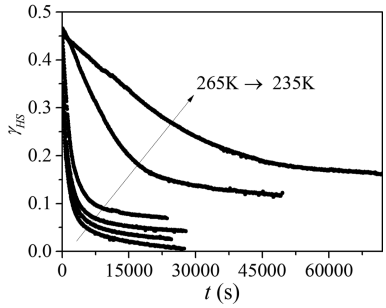

Figure 4. Isothermal relaxation curves for the HS fraction (γ_{HS}) for **1** at 265, 260, 255, 250, 240, and 235 K.

desired temperature, exhibit sigmoidal character below 245 K but deviate from this behavior at higher temperatures, due to the self-accelerating nature of the relaxation curves above T_{TIESST}. Thus, the plots cannot be satisfactorily modeled with a unique relaxation process (sigmoidal or stretch exponential). From the relaxation rate at very long times, as extracted from the linear decay of the plot tails (Figure S9), we can estimate relaxation times as long as 8 h at 265 K, and over 3 days at 235 K. We assign such striking features to the effect of multiple anionic sulfate groups in the ligand's backbone. The thermodynamically favored HS→LS process is slowed down due to the need to overcome a large activation energy arising from the electrostatic repulsion between sulfate groups on adjacent triazoles bridges. The smaller size of the LS ground state forces shorter intramolecular distances among them.

The ^{57}Fe Mössbauer data are in good agreement with the magnetic measurements. Both spectra at 295 and 4 K (Figure 5a,b) show two quadrupole doublets: one with higher quadrupole splitting (QS) due to HS Fe^{II} (Table S3) and the

DOI: 10.1021/jacs.5b07879
J. Am. Chem. Soc. 2015, 137, 11924−11927

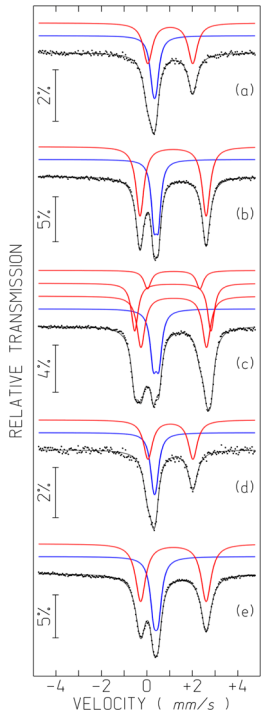

Figure 5. ^{57}Fe Mössbauer spectra of **1**: pristine sample taken at (a) 295 and (b) 4 K; sample heated at 403 K and quenched in liquid N_2, taken at (c) 4 and (d) 295 K; sample warmed up at 295 K for 24 h and taken at (e) 4 K. The blue and red lines refer to LS and HS Fe^{II}, respectively.

other with lower QS typical of LS Fe^{II}.[1] At 4 K the recoil-free fractions of LS and HS Fe^{II} are usually similar, and their relative areas may be considered a good approximation of the LS and HS Fe^{II} fractions. The slightly higher LS Fe^{II} relative area at 295 K may be attributed to its higher recoil-free fraction at 295 K. The ratio of the relative areas at 4 K, 2:1 within experimental accuracy, is consistent with the HS-LS-HS ground state in the 295−4 K temperature range.

In order to study the thermally trapped metastable HS-HS-HS state, we heated a sample at 403 K during 5 h, dropped it quickly into liquid nitrogen, and brought it to the cryostat. The spectrum obtained at 4 K (Figure 5c) showed that the relative area of the LS Fe^{II} doublet was reduced approximately 10% relative to that of the pristine sample (Table S3). In addition, the HS Fe^{II} contribution could only be fitted if three doublets were considered: a first doublet (d1) with parameters similar to those of terminal HS Fe^{II} in the untreated sample; a second doublet (d2) with a relative area of ∼11% that could be assigned to central HS Fe^{II} (notice that 11% is within experimental accuracy equal to the relative area reduction of the central LS Fe^{II}); and a third doublet (d3), with the highest QS, which may be attributed to terminal HS Fe^{II} with a modified environment. These terminal HS Fe^{II} with the highest QS are most likely the nearest Fe neighbors of the central HS Fe^{II}, in agreement with the fact that the relative area of d3 is approximately twice that of d2 and the sum of d1 and d3 relative areas is equal to the area of the HS doublet in the untreated sample. Thus, the three HS contributions to the spectra arise from the configurations HS(d1)-LS-HS(d1) and HS(d3)-HS(d2)-HS(d3). These results indicate quenching of one-third of the molecules in this experiment. The spectrum taken after warming the quenched sample to room temperature is identical, within experimental error, to the spectrum of the pristine sample (Figure 5 and Table S3), showing that the thermally quenched state decays at room temperature toward the ground state. The spectrum taken at 4 K of the treated sample after warming to room temperature for 24 h is identical to that of the untreated sample, confirming perfect stability and bistability.

In summary, we have isolated a polyanionic Fe^{II} trimer that exhibits spin-crossover behavior for its central Fe^{II} position above room temperature with a large thermal hysteresis. Transition dynamics are remarkably slow, allowing for an easy trapping of the excited spin state when the material is cooled down at reasonably slow rates (>5 K min^{-1}). As a result, this material exhibits bistability in the high-temperature range (280−400 K), but also in the low-temperature range (2−250 K), since the metastable HS state cannot relax back to the ground state up to very high temperatures (T_{TIESST} = 250 K). This is the highest temperature at which memory effect remains in a thermally quenched SCO system, even higher than the values displayed by Prussian blue analogues, where electron-transfer kinetics play a role in the stabilization of the metastable state.[44] The extremely slow relaxation exhibited at such high temperatures opens unique possibilities for room-temperature applications.

■ ASSOCIATED CONTENT

Supporting Information

The Supporting Information is available free of charge on the ACS Publications website at DOI: 10.1021/jacs.5b07879.

Crystallographic data for **1** (CIF)
Experimental methods and additional characterization data (PDF)

■ AUTHOR INFORMATION

Corresponding Author

*jrgalan@iciq.es

Present Address

[¶]V.G.: Institute of Nanotechnology, Karlsruhe Institute of Technology (KIT), Hermann-von-Helmholtz-Platz 1, 76344 Eggenstein-Leopoldshafen, Germany

Author Contributions

[#]V.G. and C.S.d.P. contributed equally.

Notes

The authors declare no competing financial interest.

■ ACKNOWLEDGMENTS

We acknowledge financial support from the EU (ERC Stg grant 279313, CHEMCOMP), the Spanish Ministerio de Economía y Competitividad (MINECO) through Severo Ochoa Excellence Accreditation 2014-2018 (SEV-2013-0319), and the ICIQ Foundation.

■ REFERENCES

(1) Gütlich, P.; Garcia, Y.; Goodwin, H. A. *Chem. Soc. Rev.* **2000**, *29*, 419−427.
(2) Bousseksou, A.; Molnar, G.; Salmon, L.; Nicolazzi, W. *Chem. Soc. Rev.* **2011**, *40*, 3313−3335.
(3) Munoz, M. C.; Real, J. A. *Coord. Chem. Rev.* **2011**, *255*, 2068−2093.
(4) Aromí, G.; Barrios, L. A.; Roubeau, O.; Gamez, P. *Coord. Chem. Rev.* **2011**, *255*, 485−546.
(5) Halcrow, M. A. *Chem. Soc. Rev.* **2011**, *40*, 4119−4142.

DOI: 10.1021/jacs.5b07879
J. Am. Chem. Soc. 2015, 137, 11924−11927

(6) Gütlich, P. *Eur. J. Inorg. Chem.* **2013**, *2013*, 581−591.
(7) Quintero, C. M.; Félix, G.; Suleimanov, I.; Sánchez Costa, J.; Molnar, G.; Salmon, L.; Nicolazzi, W.; Bousseksou, A. *Beilstein J. Nanotechnol.* **2014**, *5*, 2230−2239.
(8) Costa, J. S.; Rodríguez-Jiménez, S.; Craig, G. A.; Barth, B.; Beavers, C. M.; Teat, S. J.; Aromí, G. *J. Am. Chem. Soc.* **2014**, *136*, 3869−3874.
(9) Prins, F.; Monrabal-Capilla, M.; Osorio, E. A.; Coronado, E.; van der Zant, H. S. J. *Adv. Mater.* **2011**, *23*, 1545−1549.
(10) Miyamachi, T.; Gruber, M.; Davesne, V.; Bowen, M.; Boukari, S.; Joly, L.; Scheurer, F.; Rogez, G.; Yamada, T. K.; Ohresser, P.; Beaurepaire, E.; Wulfhekel, W. *Nat. Commun.* **2012**, *3*, 938.
(11) Gopakumar, T. G.; Matino, F.; Naggert, H.; Bannwarth, A.; Tuczek, F.; Berndt, R. *Angew. Chem., Int. Ed.* **2012**, *51*, 6262−6266.
(12) Ohkoshi, S.; Imoto, K.; Tsunobuchi, Y.; Takano, S.; Tokoro, H. *Nat. Chem.* **2011**, *3*, 564−569.
(13) Samanta, S.; Demesko, S.; Dechert, S.; Meyer, F. *Angew. Chem.* **2015**, *54*, 583−587.
(14) Sessoli, R.; Powell, A. *Coord. Chem. Rev.* **2009**, *253*, 2328−2341.
(15) Bogani, L.; Wernsdorfer, W. *Nat. Mater.* **2008**, *7*, 179−186.
(16) Matsumoto, T.; Newton, G. N.; Shiga, T.; Hayami, S.; Matsui, Y.; Okamoto, H.; Kumai, R.; Murakami, Y.; Oshio, H. *Nat. Commun.* **2014**, *5*, 3865.
(17) Aravena, D.; Ruiz, E. *J. Am. Chem. Soc.* **2012**, *134*, 777−779.
(18) Craig, G. A.; Roubeau, O.; Aromí, G. *Coord. Chem. Rev.* **2014**, *269*, 13−31.
(19) Warner, B.; Oberg, J. C.; Gill, T. G.; El Hallak, F.; Hirjibehedin, C. F.; Serri, M.; Heutz, S.; Arrio, M.-A.; Sainctavit, P.; Mannini, M.; Poneti, G.; Sessoli, R.; Rosa, P. J. *J. Phys. Chem. Lett.* **2013**, *4*, 1546−1552.
(20) Larionova, J.; Salmon, L.; Guari, Y.; Tokarev, A.; Molvinger, K.; Molnar, G.; Bousseksou, A. *Angew. Chem., Int. Ed.* **2008**, *47*, 8236−8240.
(21) Wang, C.-F.; Li, R.-F.; Chen, X.-Y.; Wei, R.-J.; Zheng, L.-S.; Tao, J. *Angew. Chem., Int. Ed.* **2015**, *54*, 1574−1577.
(22) Koo, Y.-S.; Galan-Mascaros, J. R. *Adv. Mater.* **2014**, *26*, 6785−6789.
(23) Duriska, M. B.; Neville, S. M.; Moubaraki, B.; Cashion, J. A.; Halder, G. J.; Chapman, K. W.; Balde, C.; Letard, J. F.; Murray, K. S.; Kepert, C. J.; Batten, S. R. *Angew. Chem., Int. Ed.* **2009**, *48*, 2549−2552.
(24) Hernández, E. M.; Quintero, C. M.; Kraieva, O.; Thibault, C.; Bergaud, C.; Salmon, L.; Molnar, G.; Bousseksou, A. *Adv. Mater.* **2014**, *26*, 2889−2893.
(25) Phan, H.; Benjamin, S. M.; Steven, E.; Brooks, J. S.; Shatruk, M. *Angew. Chem., Int. Ed.* **2015**, *54*, 823−827.
(26) Ludwig, E.; Naggert, H.; Kalläne, M.; Rohlf, S.; Kröger, E.; Bannwarth, A.; Quer, A.; Rossnagel, K.; Kipp, L.; Tuczek, F. *Angew. Chem., Int. Ed.* **2014**, *53*, 3019−3023.
(27) Seredyuk, M.; Muñoz, M. C.; Castro, M.; Romero-Morcillo, T.; Gaspar, A. B.; Real, J. A. *Chem. - Eur. J.* **2013**, *19*, 6591−6596.
(28) Money, V. A.; Carbonera, C.; Elhaïk, J.; Halcrow, M. A.; Howard, J. A. K.; Letard, J.-F. *Chem. - Eur. J.* **2007**, *13*, 5503−5514.
(29) Gomez, V.; Benet-Buchholz, J.; Martin, E.; Galan-Mascaros, J. R. *Chem. - Eur. J.* **2014**, *20*, 5369−5379.
(30) Gomez, V.; Lillo, V.; Escudero-Adan, E. C.; Martin, E.; Galan-Mascaros, J. R. *Dalton Trans.* **2013**, *42*, 6374−6380.
(31) Halcrow, M. A. *Chem. Lett.* **2014**, *43*, 1178−1188.
(32) Lochenie, C.; Bauer, W.; Railliet, A. P.; Schlamp, S.; Garcia, Y.; Weber, B. *Inorg. Chem.* **2014**, *53*, 11563−11572.
(33) Weber, B.; Bauer, W.; Pfaffeneder, T.; Dirtu, M. M.; Naik, A. D.; Rotaru, A.; Garcia, Y. *Eur. J. Inorg. Chem.* **2011**, *2011*, 3193−3206.
(34) Weber, B.; Bauer, W.; Obel, J. *Angew. Chem., Int. Ed.* **2008**, *47*, 10098−10101.
(35) Bushuev, M. B.; Daletsky, V. A.; Pishchur, D. P.; Gatilov, Y. V.; Korolkov, I. V.; Nikolaenkova, E. B.; Krivopalov, V. P. *Dalton Trans.* **2014**, *43*, 3906−3910.
(36) Brooker, S. *Chem. Soc. Rev.* **2015**, *44*, 2880−2892.
(37) Kulmaczewski, R.; Olguín, J.; Kitchen, J. A.; Feltham, H. L. C.; Jameson, G. N. L.; Tallon, J. L.; Brooker, S. *J. Am. Chem. Soc.* **2014**, *136*, 878−881.
(38) Murnaghan, K. D.; Carbonera, C.; Toupet, L.; Griffin, M.; Dirtu, M. M.; Desplanches, C.; Garcia, Y.; Collet, E.; Letard, J.-F.; Morgan, G. G. *Chem. - Eur. J.* **2014**, *20*, 5613−5618.
(39) Garcia, Y.; Ksenofontov, V.; Mentior, S.; Dirtu, M.; Gieck, C.; Bhatthacharjee, A.; Gütlich, P. *Chem. - Eur. J.* **2008**, *14*, 3745−3758.
(40) Craig, G. A.; Sánchez Costa, J.; Roubeau, O.; Teat, S. J.; Aromí, G. *Chem. - Eur. J.* **2011**, *17*, 3120−3127.
(41) Craig, G. A.; Costa, J. S.; Roubeau, O.; Teat, S. J.; Shepherd, H. J.; Lopes, M.; Molnar, G.; Bousseksou, A.; Aromí, G. *Dalton Trans.* **2014**, *43*, 729−737.
(42) Paradis, N.; Chastanet, G.; Letard, J. F. *Eur. J. Inorg. Chem.* **2012**, *2012*, 3618−3624.
(43) Wang, H.; Sinito, C.; Kaiba, A.; Costa, J. S.; Desplanches, C.; Dagault, P.; Guionneau, P.; Letard, J.-F.; Négrier, P.; Mondieig, D. *Eur. J. Inorg. Chem.* **2014**, *2014*, 4927−4933.
(44) Li, D.; Clerac, R.; Roubeau, O.; Harté, E.; Mathoniere, C.; Le Bris, R.; Holmes, S. M. *J. Am. Chem. Soc.* **2008**, *130*, 252−258.

DOI: 10.1021/jacs.5b07879
J. Am. Chem. Soc. 2015, 137, 11924−11927